Journal of Magnetics 16(3), 263-267 (2011) http://dx.doi.org/10.4283/JMAG.2011.16.3.263

Considerations on Improvement of Moving Properties for Magnetic Actuator Capable of Movement in Pipe

Tomohiro Izumikawa and Hiroyuki Yaguchi*

Tohoku Gakuin University, Faculty of Engineering, 1-13-1 Chuo, Tagajo, Miyagi, Japan

(Received 17 May 2011, Received in final form 21 June 2011, Accepted 24 June 2011)

The present paper proposes a novel cableless magnetic actuator with a new propulsion module that exhibits a very high thrusting force. This actuator contains an electrical inverter that directly transforms DC from button batteries into AC. The electrical DC-AC inverter incorporates a mass-spring system, a reed switch, and a curved permanent magnet that switches under an electromagnetic force. The actuator is moved by the inertial force of the mass-spring system due to mechanical resonance energy. The experimental results show that the actuator is able to move upward at a speed of 33 mm/s when using 10 button batteries when pulling a 10 g load mass. This cableless magnetic actuator has several possible applications, including narrow-pipe inspection and maintenance.

Keywords : cableless magnetic actuator, pipe inside mover, electrical DC-AC inverter, propulsion module, inertial force

1. Introduction

Finding damage inside pipes is important for the inspection of complex pipes used in nuclear power plants and chemical plants. A number of studies [1-6] have addressed mechanisms of an actuator with an electric cable to provide locomotion in the pipe by means of various devices. The design of the cable type robot is quite simple compared to the design of the cableless robot. Consequently, there are few examples of research on cableless actuators [7, 8].

The present authors previously proposed [8] a novel cableless magnetic actuator that provides propulsion by means of the inertial force of a mass-spring system excited by an electromagnetic force. Since a large-amplitude vibration can be easily provided by a small excitation force, this type of actuator has high propulsion.

The purpose of the present study is to improve the moving characteristics of the cableless magnetic actuator presented in the previous paper [8]. In order to improve the moving characteristics of the actuator, an increase in magnetic force by the application of a new propulsion module was achieved. In addition, this cableless magnetic actuator contains an electrical inverter that directly transforms DC supplied from button batteries into AC. The electrical DC-AC inverter is composed of a reed switch and a curved permanent magnet that switches under an electromagnetic force. The propulsion of this cableless magnetic actuator exhibits good performance compared with other types of actuators that are powered by an electric cable [1-6]. It was shown that this actuator is one of important magnetic application.

*Corresponding author: Tel: +81 223687104
Fax: +81 223687070, e-mail: yaguchi@tjcc.tohoku-gakuin.ac.jp

2. Cableless Magnetic Actuator

Fig. 1 is a diagram of the cableless magnetic actuator capable of moving within a pipe having an inner diameter of 8 mm. The magnetic actuator consists of two identical ring type permanent magnets, two translational springs, a bobbin type electromagnet, and an electrical DC-AC inverter composed of a reed switch and a curved permanent magnet. The ring type permanent magnet is an NdFeB magnet that is magnetized in the axial direction. The magnet has an outer diameter of 7.8 mm, an inner diameter of 5.8 mm, and a thickness of 4.5 mm.

The surface magnetic flux density measured using a tesla meter is 225 mT. The two identical translational springs are of the stainless steel compression coil type and have an outer diameter of 6 mm, a free length of 5

ⓒ 2011 Journal of Magnetics

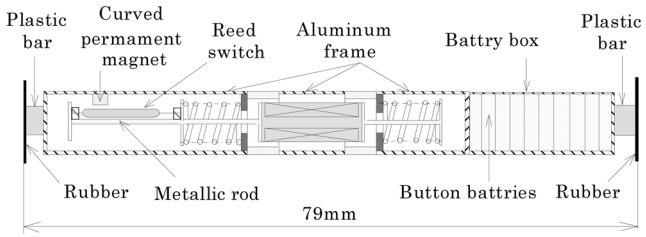

Fig. 1. Structure of the cableless magnetic actuator.

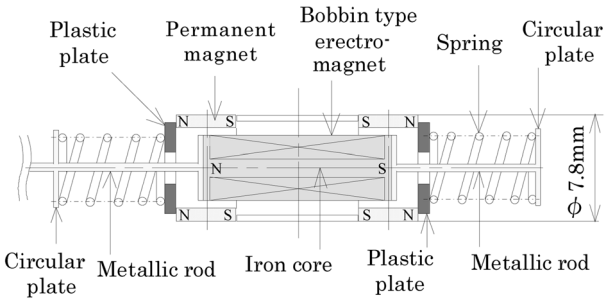

Fig. 2. Propulsion module of the actuator.

mm, and a spring constant of k = 261 N/m. The bobbin type electromagnet is composed of an iron core with 3200 turns of 0.07 mm diameter copper wire. The electrical resistance of the electromagnet is 225 Ω. This electromagnet also achieves duty of the mass of a mass-spring system by combining the two translational springs. As shown in Fig. 2, the spring is glued to a plastic plate, and the electromagnet and the two springs are connected by two metallic rods with circular plates at both ends. The ring type permanent magnets were then combined with a frame. The legs used to support the actuator are constructed from natural rubber and have a length of 12 mm, a width of 3 mm, and a thickness of 0.5 mm. The leg was attached to the frame by a square plastic bar having a length of 6 mm. The actuator, which houses 10 button batteries, has a length of 79 mm and a total mass of 8.2 g.

In addition, reversible motion of the actuator can be achieved by using several coils arranged outside the pipe, as shown in previous paper [8].

3. Principle of Locomotion

As shown in Fig. 3(a), the two rubber legs are deformed when the actuator is inserted into the pipe. In the following, we consider one period τ of vibration. The principle of locomotion for the actuator is as follows:

1) For the region $0 < \tau < t$ /4, as shown in Fig. 3(a), the rubber legs can slide due to the inertial force of the vibrating mass when the mass of the mass-spring system

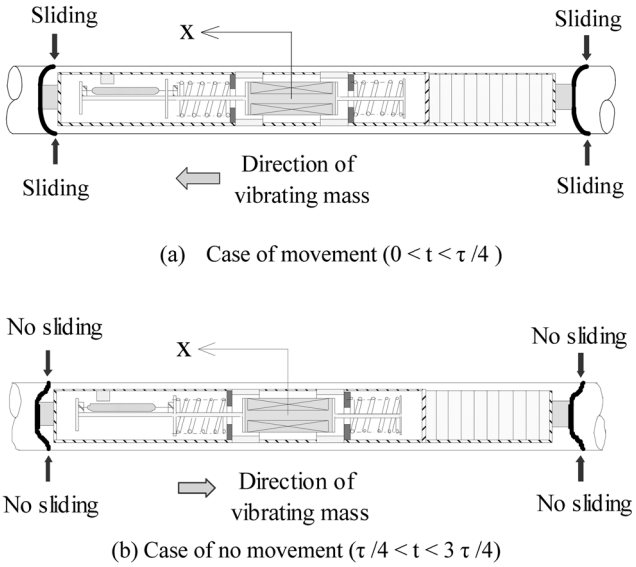

Fig. 3. Principle of locomotion.

vibrates in the x direction.

2) For the region $\tau/4 < t < 3\tau/4$, as shown in Fig. 3(b), the tips of the rubber legs are fastened to the wall inside the pipe when the vibrating mass moves in the negative x direction. The frictional force between the two rubber legs and the inner wall of the pipe becomes rather large compared with the inertial force of the vibrating mass. Therefore, the actuator can not be moved.

3) For the region $3\tau/4 < t < 4\tau/4$, the vibrating mass maintains the harmonic vibration and returns to the origin.

As a result, the actuator can only move in the x direction due to the inertial force of the vibrating mass of the mass-spring system. Thus, the actuator is propelled by the difference in the frictional force between the forward and backward motion of the two rubber legs.

4. High Propulsion by Improving the Magnetic Circuit

As mentioned above, the propulsion module of this magnetic actuator must generate a stronger excitation

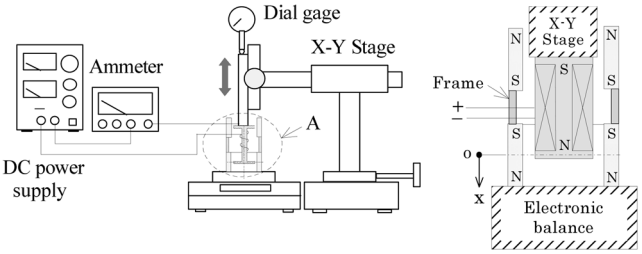

(a) Measurement of magnetic force (b) Detail of section A

Fig. 4. Experimental apparatus.

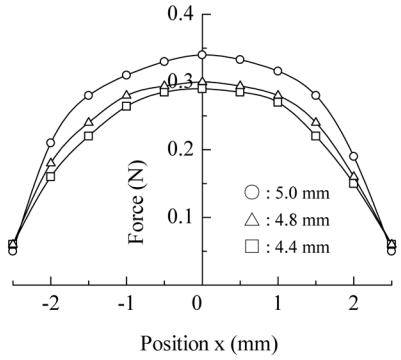

(a) H = 0.5 mm

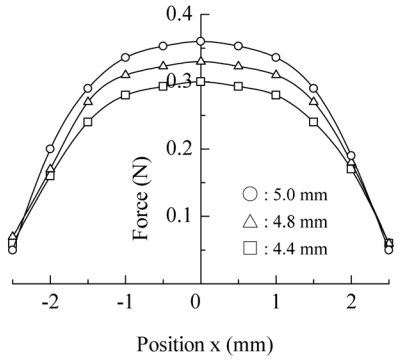

(b) H = 1.0 mm

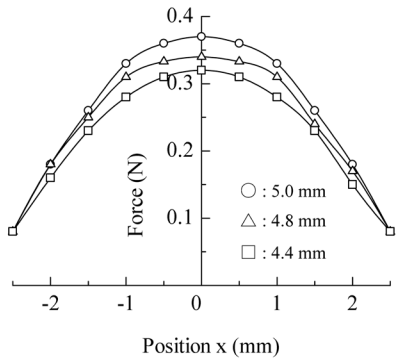

(c) H = 1.5 mm

Fig. 5. Relationship between position and static force.

force.

Before the cableless magnetic actuator was fabricated, the static characteristics for the propulsion module of the magnetic actuator were examined. A magnetic circuit composed of two identical ring type permanent magnets and a bobbin type electromagnet was tested. The iron core of the bobbin type electromagnet consists of two identical circular plates of diameter D (mm) and thickness H (mm) and a straight rod of 2.5 mm in diameter, as shown in Fig. 2. The iron core with the integral structure was machined using a lathe. An experimental test was conducted using the apparatus shown in Fig. 4(a). A direct current of 0.05 A was applied to the electromagnet during measurement. The origin of the measurement was taken as center of the ring type permanent magnet, and the position x was measured as shown in Fig. 4(b).

Fig. 5 shows the relationship between the position x and the static force measured by a force gage with respect to the iron core having diameters D of 4.4, 4.8, and 5 mm and thicknesses H of the iron core of 0.5, 1, and 1.5 mm, respectively. In the experiment, the static force was measured for only one circular plate of the iron core and the obtained result was doubled. The maximum static force was 0.37 N for the case in which H = 1.5 mm and D = 5 mm. On the other hand, the maximum static force was 0.36 N for H = 1 mm and D = 5 mm. Since the difference in maximum static force was slight among the investigated cases, the iron core with a circular plate with H = 1 mm and D = 5 mm was used in the present study.

For the propulsion module used in the previous paper [8], the maximum static force was 0.2 N when a direct current of 0.05 A was applied to the electromagnet. Thus, the measured maximum static force in the present experiment was 1.8 times greater than that in the previous paper [8].

5. Structure and Operating Principle of the Electrical DC-AC Inverter

Fig. 6 shows an outline of the electrical DC-AC inverter proposed in the present paper in order to realize the

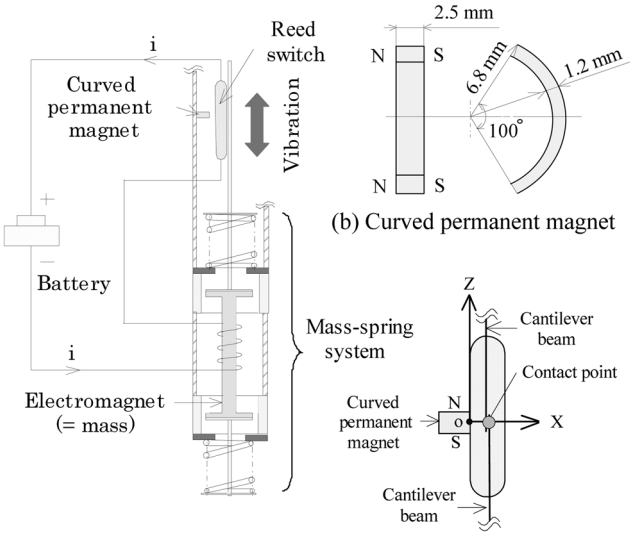

(a) Principle of the DC-AC inverter (c) Reed switch

Fig. 6. Principle of the electrical DC-AC inverter composed of a reed switch and a curved permanent magnet.

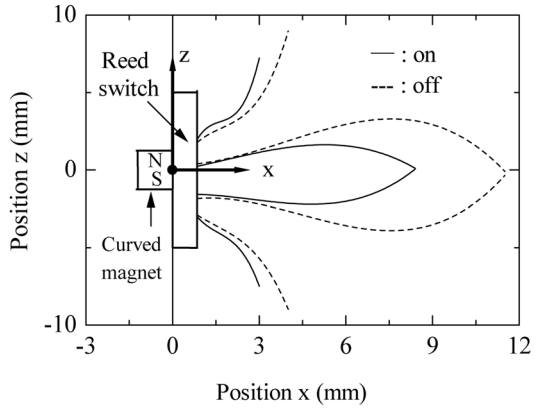

Fig. 7. On-off area of the reed switch around the curved permanent magnet.

cableless actuator. Considering durability, the mechanical DC-AC inverter demonstrated in the previous paper [8] was exchanged for an electric inverter. The electric inverter is composed of a reed switch and a curved permanent magnet, as mentioned above. The reed switch is 1.8 mm in diameter and has a length of 10 mm. The curved permanent magnet is an arc type NdFeB magnet of 1.2 mm in width and 2.5 mm in thickness and is magnetized in the axial direction. The reed switch and the bobbin type electromagnet are connected by a thin copper wire to a DC source, such as a battery, as shown in Fig. 6(a). The reed switch attached to the electromagnet vibrates around the curved permanent magnet. The strength and weakness of the magnetic field between the curved permanent magnet and the reed switch attached on the mass by the vibration displacement of the mass-spring system is generated. The mass-spring system vibrates, and the two cantilever beams inserted in the reed switch make and break contact as the switch is cycled on and off. As a result, the DC voltage is converted into a square alternating waveform, and the magnetic force operates on the mass-spring system.

The DC source for the experiment was composed of ten SR621W silver-oxide button batteries. When the electromagnet was connected to the battery pack, the direct current into the electromagnet was 0.05 A. Fig. 6(b) and 6(c) show in detail the arrangement of the reed switch and the curved permanent magnet. The origin of the measurement was taken as the center of the curved permanent magnet, and the x and z coordinates, which are shown in relation to the left-hand side of the reed switch, were measured as shown in this figure.

Fig. 7 shows the on-off area of the reed switch around the curved permanent magnet. In this figure, the center point indicates the contact point of the two cantilever beams inserted into the reed switch. The solid line indicates the on-area of the reed switch, and the broken line indicates the off-area.

6. Locomotion Characteristics of the Cableless Magnetic Actuator

In this actuator, position x between the reed switch and the curved magnet is 5.3 mm, and position z is 3.2 mm. Consequently, the duty factor of the square wave produced by the inverter module is 35%. The effective value of the alternating current into the electromagnet is 18 mA. Ten SR621W silver-oxide button batteries (Maxell) were used as the power source for the actuator. The completely fabricated actuator was then inserted into an acrylic pipe with an inner diameter of 8 mm. The driving frequency of this magnetic actuator was 100 Hz. The solid line in Fig. 8 shows the relationship between the tilt angle and the speed of the actuator. The tilt angle α was varied from $\alpha = -90°$ (straight down) to $\alpha = 90°$ (straight up). With 10 batteries, the maximum vertical upward speed was 68.7 mm/s when the supporting force F of the actuator was

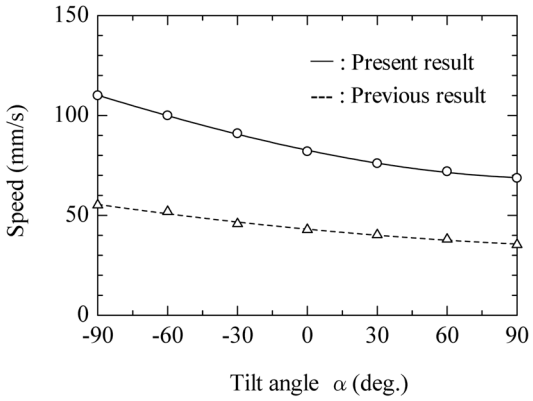

Fig. 8. Relationship between tilt angle and speed.

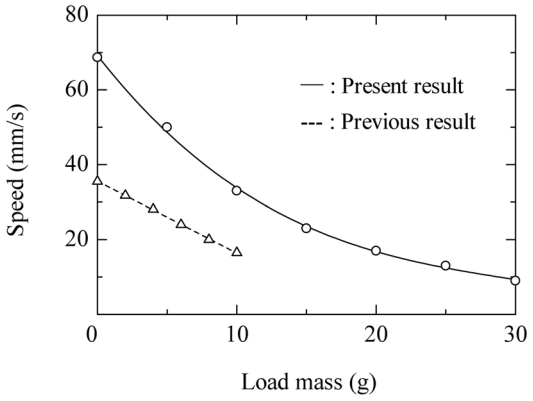

Fig. 9. Relationship between load mass and vertical speed upward.

0.25 N. The broken line in Fig. 8 shows the results of the previous study [8]. It can be seen that the maximum vertical upward speed in the present study is about 2 times higher than that previously obtained [8], which is high for a cableless actuator. The moving characteristics of the actuator have improved considerably by the improvement of the magnetic circuit. This actuator demonstrates good performance compared with actuators powered by electric cable.

The solid line in Fig. 9 shows the relationship between the load mass and the speed when moving straight up using 10 button batteries. The figure indicates that the actuator was able to climb at 17 mm/s when pulling a load mass of 20 g, which is moderately good performance. In this figure, the broken line shows the results obtained in the previous study [8]. Thus, the propulsion characteristics were improved considerably.

7. Conclusion

A cableless magnetic actuator powered by an electrical DC-AC inverter and capable of locomotion in a thin pipe has been proposed and tested. The actuator exhibited a speed of 82 mm/s when moving horizontally and a speed of 68.7 mm/s when moving straight upward. The total range of the actuator was 128 m in the horizontal direction and 107 m in the vertical direction over 26 min when the supporting force of the actuator was 0.25 N. If the power requirement of the propulsion module can be reduced, it may be possible to extend the range to several hundred meters.

This cableless magnetic actuator has several possible applications, including pipe inspection and maintenance by attaching a micro-camera to it.

References

[1] H. Saito, K. Sato, K. Kudo, and K. Sato, Trans. Japan Soc. Mech. Eng. **66**, 641 (2000).
[2] M. Ohno, T. Hamano, and S. Kato, Journal of Robotics and Mechatoronics **18**, 1 (2006).
[3] Y. Kondo and S. Yokota, Trans. Japan Soc. Mech. Eng. **64**, 617 (1998).
[4] S. Guo and Q. Pan, Proc., IEEE/RSJ International Conference on Intelligent Robots and Systems, 2265 (2005).
[5] T. Miyagawa and N. Iwatski, Journal of the Japan Society for Precision Engineering **74**, 12 (2008).
[6] K. Suzumori, S. Wakimoto, and M. Tanaka, Proc., IEEE International Conf. Robotics and Automation, 2735 (2003).
[7] K. Tsuruta, T. Shibata, N. Mitsumoto, T. Sasaya, and M. Kawahara, Trans. IEE Jpn. **122**, 2 (2002).
[8] H. Yaguchi, K. Ishikawa, and T. Zamma, IEEE Trans. Magn. **45**, 10 (2009).